

Investigation for $D^+ \rightarrow \pi^+ \nu \bar{\nu}$ decay process within QCDSR approach

Yu Chen, Hai-Bing Fu,^{*} Tao Zhong,[†] and Sheng-Bo Wu
Department of Physics, Guizhou Minzu University, Guiyang 550025, P.R.China

Dong Huang

Center of Experimental Training, Guiyang Institute of Information Science and Technology, Guiyang 550025, P.R.China
 (Dated: January 9, 2024)

In the paper, we investigate the charmed meson rare decay process $D^+ \rightarrow \pi^+ \nu \bar{\nu}$ by using QCD sum rules approach. Firstly, the pion twist-2 and twist-3 distribution amplitude ξ -moments $\langle \xi_{2;\pi}^n \rangle|_\mu$ up to 10th-order and $\langle \xi_{3;\pi}^{(p,\sigma),n} \rangle|_\mu$ up to fourth-order are calculated by using QCD sum rule under background field theory. After constructing the light-cone harmonic oscillator model for pion twist-2, 3 DAs, we get their behaviors by matching the calculated ξ -moments. Then, the $D \rightarrow \pi$ transition form factors are calculated by using QCD light-cone sum rules approach. The vector form factor at large recoil region is $f_+^{D \rightarrow \pi}(0) = 0.627_{-0.080}^{+0.120}$. By taking the rapidly $z(q^2, t)$ converging simplified series expansion, we present the TFFs and the corresponding angular coefficients in the whole squared momentum transfer physical region. Furthermore, we display the semileptonic decay process $\bar{D}^0 \rightarrow \pi^+ e \bar{\nu}_e$ differential decay widths and branching fraction with $\mathcal{B}(\bar{D}^0 \rightarrow \pi^+ e \bar{\nu}_e) = 0.308_{-0.066}^{+0.155} \times 10^2$. The $\bar{D}^0 \rightarrow \pi^+ e \bar{\nu}_e$ differential/total predictions for forward-backward asymmetry, q^2 -differential flat terms and lepton polarization asymmetry are also given. After considering the non-standard neutrino interactions, the predictions for the $D^+ \rightarrow \pi^+ \nu \bar{\nu}$ branching fraction is $\mathcal{B}(D^+ \rightarrow \pi^+ \nu \bar{\nu}) = 1.85_{-0.46}^{+0.93} \times 10^{-8}$.

PACS numbers: 13.25.Hw, 11.55.Hx, 12.38.Aw, 14.40.Be

I. INTRODUCTION

The remarkable success of Standard Model (SM) in describing all current experimental information suggests that the search for deviations from it should focus on either higher energy scales or small effects in low energy observables.[1]. Normally, the flavour changing neutral current (FCNC) transitions in the SM are highly suppressed by the Glashow-Iliopoulos-Maiani (GIM) mechanism [2]. This GIM suppression has more strongly effective in charm sector compared to the down-type quarks in the bottom and strange sectors. Meanwhile, the suppression is responsible for the relatively small size of charm mixing and CP violation in the charm system [3–5]. So the FCNC processes of D -meson decays into charged lepton pairs are always totally overshadowed by long-distance contributions [6, 7]. However, for D -meson FCNC decays into final states involving dineutrinos, such as $D^+ \rightarrow \pi^+ \nu \bar{\nu}$, long-distance contributions become insignificant and the short-distance contributions from Z -penguin and box diagrams are dominant, which results in the branching fraction at the level of 10^{-16} in SM [8]. That makes D -meson FCNC decay involving dineutrinos a unique and clean probe to study the CP violation in the charm sector [9] and search for new physics beyond SM [10].

On the experimental side, LHCb Collaboration reported an evidence for the breaking of lepton univer-

sality in bottom-quark FCNC decays to charged dielectrons and dimuons with a significance of 3.1σ [11], which suggests the possible presence of new physics contributions in the lepton sector [12]. The neutral charmed meson FCNC decay into dineutrinos pair have been observed by the BESIII Collaboration, which provide the upper limits at 10% confidence level for the $D^0 \rightarrow \pi^0 \nu \bar{\nu}$ branching fraction, i.e. 2.1×10^{-4} in 2021 [13]. This value is much larger than the SM prediction both from the long-distance and short distance. Non-standard neutrino interactions (NSIs) [14–24], which described by four fermion operators of the $(\bar{\nu}_\alpha \gamma \nu_\beta)(\bar{f} \gamma f)$ can narrow the gap between the experimental and the SM's predictions. It has been shown that the NSIs would be compatible with the oscillation effects along with some new features in various neutrino searches [25–31]. Meanwhile, NSIs are thought to be well matched with the oscillation effects, along with new features in neutrino searches [32–38]. The branching ratio of $D^+ \rightarrow \pi^+ \nu \bar{\nu}$ could be at the level 10^{-8} . This approach can establish $D^+ \rightarrow \pi^+ \nu \bar{\nu}$ direct connection with $\bar{D}^0 \rightarrow \pi^+ e \bar{\nu}_e$, which lead to the motivation in this paper.

The $D \rightarrow \pi$ transition form factors (TFFs) are the key component of semileptonic decays $\bar{D}^0 \rightarrow \pi^+ e \bar{\nu}_e$. There are some researches dealing with the $D \rightarrow \pi$ TFFs both from experimental and theoretical side. Experimentally, the Belle [39], BESIII [40], BABAR [41], CLEO [42] Collaborations have measured the vector TFFs value at large recoil region $f_+^{D \rightarrow \pi}(0)$. Meanwhile, the Lattice QCD also give this value [43]. Theoretically, the $D \rightarrow \pi$ TFFs can be calculated by using the QCD light-cone sum rule (LCSR) [44], light-front quark model (LFQM) [45], combined heavy meson and chiral Lagrangian theory

^{*}Electronic address: fuhb@gzmu.edu.cn

[†]Electronic address: zhongtao1219@sina.com

HM χ T [46]. The LCSR approach is mainly extension on the light cone, which is expected to be valid at small and intermediate squared momentum transfer. After extrapolating the TFFs by using a suitable series expansion, one can get the vector and scalar TFFs in the whole physical region. Then one can make a comparison with other approaches. So in this paper, we mainly take the LCSR method to calculate the $D \rightarrow \pi$ TFFs.

Furthermore, the pion DAs with different twist structures are the key long-distance nonperturbative component in $D \rightarrow \pi$ TFFs LCSR expressions, which describes either contributions of the transverse motion of quarks (antiquarks) in the leading-twist components or contributions of higher Fock states with additional gluons and/or quark-antiquark pairs. Considering the contributions for each twist DA, the leading-twist and twist-3 DAs are dominant. The higher twists DAs contributions are highly suppressed by the energy scale and Borel parameters [47, 48]. For pion leading-twist DA, there have some predictions coming from theoretical group, such as the Lattice QCD (LQCD) [49], DS model [50] and QCD/AdS model [51]. To the pion twist-3 DAs, the light-front quark model (LFQM) [52] and QCDSR [53–55] have given the predictions. To get a more better ending-point behavior of pion twist-2, 3 DAs, we will calculate the ξ -moments and reconstruct the light-cone harmonic oscillator models.

The rest of paper are organized as follows. In Sec. II, we present the NSIs and branching fraction for $D^+ \rightarrow \pi^+ \nu_\ell \bar{\nu}_{\ell'}$, the $D \rightarrow \pi$ TFFs, pion twist-2 and twist-3 LCHO model and ξ -moment within QCDSR approach. In Sec. III, we give a detailed numerical and phenomenological analysis. Finally, a brief summary is provided in Sec. IV

II. CALCULATION TECHNOLOGY

An effective four fermion interactions including neutrinos, which is called NSIs, have the following Lagrangian

$$\mathcal{L}_{\text{eff}}^{\text{NSI}} = -2\sqrt{2}G_F \varepsilon_{\ell\ell'}^{fP} (\bar{\nu}_\ell \gamma_\mu L \nu_{\ell'}) (\bar{f} \gamma^\mu P f), \quad (1)$$

where ℓ and ℓ' stand for the light neutrino flavour. The symbol f is the charged lepton or quark. $P = (L, R)$ with $L(R) = (1 \mp \gamma_5)/2$ stand for the left or right operators. $\varepsilon_{\ell\ell'}^{fP}$ is the parameter for NSIs, which carry information about dynamics. The effective Hamiltonian governing the decays $D \rightarrow \pi \nu \bar{\nu}$, resulting from the Z^0 -penguin and box-type contributions, can be written as [56]

$$\mathcal{H}_{\text{eff}} = \frac{G_F}{\sqrt{2}} \frac{\alpha}{2\pi \sin^2 \theta_W} \sum_{\ell=e,\mu,\tau} [V_{cs}^* V_{cd} X_{\text{NL}}^\ell + V_{ts}^* V_{td} X(x_t)] \times (\bar{s}d)_{V-A} (\bar{\nu}_\ell \nu_\ell)_{V-A}. \quad (2)$$

The X_{NL}^ℓ is the charm quark contribution, and $X(x_t)$ is representing the loop integral of the top quark con-

tribution. *i.e.* $X(x_t) = \eta_X x_t / 8 \times [(x_t + 2)/(x_t - 1) + (3x_t - 6)/(x_t - 1)^2 \ln x_t]$. The expressions $x_t = m_t^2/m_W^2$ and $(\bar{f}f')_{V-A} = \bar{f} \gamma_\mu (1 - \gamma_5) f'$ have been adopted. The processes are dominated by short distance because long distance contributions are almost 10^{-3} less than short distance. The up-type quark in the loop will increase the branching ratios of these reactions. The NSIs in Eq. (1) can induce the transition $c \rightarrow u \nu_\ell \bar{\nu}_{\ell'}$ at one-loop level with a Feynman diagram, as we can be obtained [56]

$$H_{c \rightarrow u \nu_\ell \bar{\nu}_{\ell'}}^{\text{NSI}} = \frac{G_F}{\sqrt{2}} \left(\frac{\alpha_{em}}{4\pi \sin^2 \theta_W} V_{cd} V_{ud}^* \varepsilon_{\ell\ell'}^{dL} \ln \frac{\Lambda}{m_W} \right) \times (\bar{\nu}_\ell \nu_{\ell'})_{V-A} (\bar{c}u)_{V-A}. \quad (3)$$

Where θ_W is the Weinberg angle, $V_{cd} = 0.225$ and $V_{ud}^* = 0.97370$. Accordingly, the branching fraction for $D^+ \rightarrow \pi^+ \bar{\nu}_\ell \nu_{\ell'}$ is given, which leads to

$$\mathcal{B}(D^+ \rightarrow \pi^+ \nu_\ell \bar{\nu}_{\ell'})_{\text{NSI}} = \left| V_{ud}^* \frac{\alpha_{em}}{4\pi \sin^2 \theta_W} \varepsilon_{\ell\ell'}^{dL} \ln \frac{\Lambda}{m_W} \right|^2 \times \mathcal{B}(\bar{D}^0 \rightarrow \pi^+ e \bar{\nu}_e) \quad (4)$$

In order to study relevant physical observables, we adopt the explicit expression for the full differential decay width distribution of $D \rightarrow \pi \ell \bar{\nu}_\ell$ as follows [57, 58]:

$$\frac{d^2 \Gamma(D \rightarrow \pi \ell \bar{\nu}_\ell)}{d \cos \theta d q^2} = a_{\theta_\ell}(q^2) + b_{\theta_\ell}(q^2) \cos \theta_\ell + c_{\theta_\ell}(q^2) \cos^2 \theta_\ell \quad (5)$$

where the three q^2 -dependent angular coefficient functions have the following expressions:

$$a_{\theta_\ell}(q^2) = \mathcal{N}_{\text{ew}} \lambda^{3/2} \left(1 - \frac{m_\ell^2}{q^2} \right)^2 \left[|f_+^{D \rightarrow \pi}(q^2)|^2 + \frac{m_\ell^2}{q^2 \lambda} \times \left(1 - \frac{m_\pi^2}{m_D^2} \right)^2 |f_0^{D \rightarrow \pi}(q^2)|^2 \right], \quad (6)$$

$$b_{\theta_\ell}(q^2) = 2\mathcal{N}_{\text{ew}} \lambda \left(1 - \frac{m_\ell^2}{q^2} \right)^2 \frac{m_\ell^2}{q^2} \left(1 - \frac{m_\pi^2}{m_D^2} \right) \times \text{Re} [f_+^{D \rightarrow \pi}(q^2) f_0^{D \rightarrow \pi^*}(q^2)], \quad (7)$$

$$c_{\theta_\ell}(q^2) = -\mathcal{N}_{\text{ew}} \lambda^{3/2} \left(1 - \frac{m_\ell^2}{q^2} \right)^3 |f_+^{D \rightarrow \pi}(q^2)|^2. \quad (8)$$

From which, the electro-weak normalized coefficient can be expressed as $\mathcal{N}_{\text{ew}} = G_F^2 |V_{cd}|^2 m_D^3 / (192 \pi^3)$ and $\lambda(a, b, c) \equiv a^2 + b^2 + c^2 - 2(ab + ac + bc)$. In this paper, we take the shorthand notations for $\lambda \equiv \lambda(1, m_\pi^2/m_D^2, q^2/m_D^2)$ for convenience. In addition, the helicity angle θ_ℓ is defined as the angle between the ℓ^- direction of flight and the final-state meson momentum in the dilepton rest frame. Thus in the massless lepton limit, we can observe two interesting algebra relations for the angular functions $b_{\theta_\ell}(q^2) = 0$ and $a_{\theta_\ell}(q^2) + c_{\theta_\ell}(q^2) = 0$.

Furthermore, we should carry out a calculation for the

$D \rightarrow \pi$ TFFs. In the first place, to derive LCSR expressions for the $D \rightarrow \pi$ TFFs, we will calculate take the standard correlator as the starting point, and then there's operator product expansion (OPE) near the light cone near zero. The vacuum-to-pion correlation function used to obtain the LCSR for the form factors of $D \rightarrow \pi$ transition is defined as:

$$\Pi_\mu(p, q) = i \int d^4x e^{iq \cdot x} \langle \pi^+(p) | T \{ j_\mu(x), j_5^\dagger(0) \} | 0 \rangle, \quad (9)$$

with the two currents $j_\mu(x) = \bar{u}(x)\gamma_\mu c(x)$ and $j_5^\dagger(0) = m_c \bar{c}(0)i\gamma_5 d(0)$. After taking the c -quark propagators into the correlation function and making operator product expansion, we can get the $D \rightarrow \pi$ TFFs OPE expression. On the other hand, after inserting hadronic states to the correlator Eq. (9), one can isolate the ground-state D -meson contributions in the dispersion relations for all three invariant amplitudes:

$$\Pi^H(p, q) = \frac{2f_+^{D \rightarrow \pi}(q^2)m_D^2 f_D}{m_c(m_D^2 - (p+q)^2)} + \int_{s_0}^\infty ds \frac{\rho(s)}{s - (p+q)^2} + \text{subtractions}. \quad (10)$$

$$\tilde{\Pi}^H(p, q) = \frac{\tilde{f}^{D \rightarrow \pi}(q^2)m_D^2 f_D}{m_c(m_D^2 - (p+q)^2)} + \int_{s_0}^\infty ds \frac{\tilde{\rho}(s)}{s - (p+q)^2} + \text{subtractions}. \quad (11)$$

The $D \rightarrow \pi$ form factors entering the residues of the D -meson pole in Eq. (11) are defined as: $\langle \pi^+(p) | \bar{u}\gamma_\mu c | \bar{D}(p+q) \rangle = 2f_+^{D \rightarrow \pi}(q^2)p_\mu + \tilde{f}^{D \rightarrow \pi}q_\mu$ with $\tilde{f}^{D \rightarrow \pi}(q^2) = f_+^{D \rightarrow \pi}(q^2) + f_-^{D \rightarrow \pi}(q^2)$. Meanwhile the $f_D = \langle D | m_c \bar{d}i\gamma_5 d | 0 \rangle / m_D^2$ is D -meson decay constant. With the help of quark-hadron duality, introducing the effective threshold parameter s_0 . After the Borel transformation in the variable $(p+q)^2 \rightarrow M^2$, the sum rules for $D \rightarrow \pi$ form factors are obtained. The LCSR for the vector form factor reads:

$$f_+^{D \rightarrow \pi}(q^2) = \frac{e^{m_D^2/M^2}}{2m_D^2 f_D} \left[F_0(q^2, M^2, s_0) + \frac{\alpha_s C_F}{4\pi} F_1(q^2, M^2, s_0) \right], \quad (12)$$

$$\tilde{f}^{D \rightarrow \pi}(q^2) = \frac{e^{m_D^2/M^2}}{m_D^2 f_D} \left[\tilde{F}_0(q^2, M^2, s_0) + \frac{\alpha_s C_F}{4\pi} \tilde{F}_1(q^2, M^2, s_0) \right], \quad (13)$$

where the LO expression for $F_0(q^2, M^2, s_0)$ and $\tilde{F}_0(q^2, M^2, s_0)$ have the following forms

$$F_0(q^2, M^2, s_0) = m_c^2 f_\pi \int_{u_0}^1 du e^{-\frac{m_c^2 - \bar{u}q^2}{uM^2}} \left\{ \frac{\phi_{2;\pi}(u, \mu)}{u} + \frac{\mu_\pi}{m_c} \left[\phi_{3;\pi}^p(u) + \left(\frac{1}{3u} - \frac{m_c^2 + q^2}{6(m_c^2 - q^2)} \frac{d}{du} \right) \times \phi_{3;\pi}^\sigma(u, \mu) \right] - 2 \left(\frac{f_{3;\pi}}{m_c f_\pi} \right) \frac{I_{3;\pi}(u)}{u} + \frac{1}{m_c^2 - q^2} \left[-\frac{m_c^2 u}{4(m_c^2 - q^2)} \frac{d^2 \phi_{4;\pi}(u)}{du^2} + u \psi_{4;\pi}(u) + \int_0^u dv \psi_{4;\pi}(v) - I_{4;\pi}(u) \right] \right\} \quad (14)$$

$$\tilde{F}_0(q^2, M^2, s_0) = m_c^2 f_\pi \int_{u_0}^1 du e^{-\frac{m_c^2 - \bar{u}q^2}{uM^2}} \left\{ \frac{\mu_\pi}{m_c} \left(\frac{\phi_{3;\pi}^p(u)}{u} + \frac{1}{6u} \frac{d\phi_{3;\pi}^\sigma(u)}{du} \right) + \frac{1}{m_b^2 - q^2} \psi_{4;\pi}(u) \right\}. \quad (15)$$

where $\mu_\pi = m_\pi^2/(m_u + m_d)$, $u_0 = (m_c^2 - q^2)/(s_0 - q^2)$ [59]. s_0 is the effective threshold parameter, f_D and f_π is decay constants of D and π -mesons, m_c is the charm quark mass. $\phi_{2;\pi}(u, \mu)$ and $\phi_{3;\pi}^p(u, \mu)$, $\phi_{3;\pi}^\sigma(u, \mu)$ are the pionic twist-2 and twist-3 DA's, respectively. While, the allowable physical range is $0 \leq q^2 \leq (m_D - m_\pi)^2 \approx 2.9 \text{ GeV}^2$. The NLO correction $F_1(q^2, M^2, s_0)$ is mainly comes from Refs. [60, 61].

Furthermore, in dealing with the pion different twist DAs especially twist-2 and twist-3 DAs, at processes related typical scale, we can take the Brodsky-Huang-Lepage (BHL) description [62], and it is the light-cone harmonic oscillator model (LCHO model) of the pion twist-2 and twist-3 WF [63, 64]. The wavefunction for

the twist-2 LCDA can be expressed as $\Psi_{2;\pi}(x, \mathbf{k}_\perp) = \sum_{\lambda_1 \lambda_2} \chi_{2;\pi}^{\lambda_1 \lambda_2}(x, \mathbf{k}_\perp) \Psi_{2;\pi}^R(x, \mathbf{k}_\perp)$ with \mathbf{k}_\perp is the pionic transverse momentum, λ_1 and λ_2 are the helicities of the two constituent quarks. $\chi_{2;\pi}^{\lambda_1 \lambda_2}(x, \mathbf{k}_\perp)$ replace the spin-space wavefunction (WF) that based on the Wigner-Melosh rotation, whose preformance for different $\lambda_1 \lambda_2$ are exhibited, which can also been seen in Refs. [65–67]. $\Psi_{2;\pi}^R(x, \mathbf{k}_\perp) = A_{2;\pi} \varphi_{2;\pi}(x) \exp[-(\mathbf{k}_\perp^2 + m_q^2)/(8\beta_{2;\pi}^2 x \bar{x})]$ with $\bar{x} = (1 - x)$. $A_{2;\pi}$ is the normalization constant, \mathbf{k}_\perp -dependence part of the spatial WF $\Psi_{2;\pi}^R(x, \mathbf{k}_\perp)$ comes from quark model of pion and confirm the WF's transverse distribution and get through the harmonious parameter $\beta_{2;\pi}$. Here we take $m_q = 250 \text{ MeV}$ in this paper. Combine with pionic leading-twist DA and WF through

the relationship:

$$\phi_{2;\pi}(x, \mu) = \frac{2\sqrt{6}}{16\pi^3 f_\pi} \int_{|\mathbf{k}_\perp|^2 \leq \mu^2} d^2\mathbf{k}_\perp \Psi_{2;\pi}(x, \mathbf{k}_\perp), \quad (16)$$

After taking the spin-space wavefunction and spatial wavefunction into the above formula, one can get the full LCHO expression for the pion leading-twist DA:

$$\begin{aligned} \phi_{2;\pi}(x, \mu) &= \frac{\sqrt{3}A_{2;\pi}m_q\beta_{2;\pi}}{2\pi^{3/2}f_\pi} \sqrt{x\bar{x}}\varphi_{2;\pi}(x) \\ &\times \left\{ \text{Erf} \left[\sqrt{\frac{m_q^2 + \mu^2}{8\beta_{2;\pi}^2 x\bar{x}}} \right] - \text{Erf} \left[\sqrt{\frac{m_q^2}{8\beta_{2;\pi}^2 x\bar{x}}} \right] \right\}. \end{aligned} \quad (17)$$

with $\varphi_{2;\pi}(x) = [x\bar{x}]^{\alpha_{2;\pi}} [1 + \hat{a}_{2;\pi}^2 C_2^{3/2}(\xi)]$ with $\xi = (2x-1)$. $\text{Erf}(x) = 2 \int_0^x e^{-t^2} dx / \sqrt{\pi}$ is the error function [68]. Meanwhile, the $\hat{a}_{2;\pi}^2$ are the second-order Gegenbauer moment, and the parameters $\alpha_{2;\pi}$ and $\hat{a}_{2;\pi}^2$ can be determined by fitting the moments $\langle \xi_{2;\pi}^n \rangle|_\mu$ directly through the method of least squares.

Meanwhile, the two pion twist-3 LCDAs can also be related to its wavefunction by using the formula

$$\phi_{3;\pi}^{p,\sigma}(x, \mu) = \frac{1}{16\pi^3} \int_{|\mathbf{k}_\perp|^2 \leq \mu^2} d^2\mathbf{k}_\perp \Psi_{3;\pi}^{p,\sigma}(x, \mathbf{k}_\perp), \quad (18)$$

Here, we take the LCHO model for pion twist-3 wavefunction. Its basic idea is the longitudinal behavior is dominated by the first two Gegenbauer moments and transverse momentum dependence the BHL prescription. In this approach, the twist-3 DA will have a better end-point behavior other than asymptotic one shall. Then, we found that the transverse momentum dependence is just in the exponential form of the off-shell energy of the constituent quarks, which agrees with Brodsky and Teramond's holographic model that is obtained by using the Anti-de Sitter (AdS) conformal field theory correspondence [69–71]. The detail discussion can be seen in our previous work [72]. Then we can obtain:

$$\begin{aligned} \phi_{3;\pi}^{p,\sigma}(x, \mu) &= \frac{A_{3;\pi}^{p,\sigma}(\beta_{3;\pi}^{p,\sigma})^2}{2\pi^2} \varphi_{3;\pi}^{p,\sigma}(x) \exp \left[-\frac{m_q^2}{8(\beta_{3;\pi}^{p,\sigma})^2 x\bar{x}} \right] \\ &\times \left\{ 1 - \exp \left[-\frac{\mu^2}{8(\beta_{3;\pi}^{p,\sigma})^2 x\bar{x}} \right] \right\}, \end{aligned} \quad (19)$$

with $\varphi_{3;\pi}^p(x) = 1 + B_{3;\pi}^p C_2^{1/2}(\xi) + C_{3;\pi}^p C_4^{1/2}(\xi)$ and $\varphi_{3;\pi}^\sigma(x) = 1 + B_{3;\pi}^\sigma C_2^{3/2}(\xi) + C_{3;\pi}^\sigma C_4^{3/2}(\xi)$. Next, we will face to the four free parameters in the LCHO model of pion twist-2 and twist-3 DAs. The first constraint is the twist-2, 3 DAs are normalized to 1. The second one is the average value of the squared transverse momentum is taken to be $(\langle \mathbf{k}_\perp^2 \rangle_{2;\pi})^{1/2} = (\langle \mathbf{k}_\perp^2 \rangle_{3;\pi}^{p,\sigma})^{1/2} = 0.35 \text{ GeV}$ [73]. Then, to determine the remaining two parameters, we need to calculate the pion DA ξ -moments which have the following definitions

$$\langle \xi_{2;\pi}^n \rangle|_\mu = \int_0^1 dx (2x-1)^n \phi_{2;\pi}(x, \mu), \quad (20)$$

$$\langle \xi_{3;\pi}^{(p,\sigma),n} \rangle|_\mu = \int_0^1 dx (2x-1)^n \phi_{3;\pi}^{(p,\sigma)}(x, \mu). \quad (21)$$

So our next task is to calculate pion twist-2, 3 DA moments by using QCD sum rule method.

In order to derive the ξ -moments of π -meson twist-2 and twist-3 DAs $\phi_{2;\pi}(x)$ and $\phi_{3;\pi}^{p,\sigma}(x)$, we take the following correlation functions

$$\begin{aligned} \Pi_{2;\pi}(z, q) &= i \int d^4x e^{iq \cdot x} \langle 0 | T \{ J_{2;\pi}^n(x), J_{2;\pi}^{0\dagger}(0) \} | 0 \rangle, \\ \Pi_{3;\pi}^{p,\sigma}(z, q) &= -i \int d^4x e^{iq \cdot x} \langle 0 | T \{ J_{3;\pi}^{(p,\sigma),n}(x), J_5^{0\dagger}(0) \} | 0 \rangle, \end{aligned} \quad (22)$$

where the twist-2 DA currents are $J_{2;\pi}^n(x) = \bar{d}(x) \not{x} \gamma_5 (iz \cdot \overleftrightarrow{D})^n u(x)$ and $J_{2;\pi}^0(x) = \bar{d}(x) \not{x} \gamma_5 u(x)$. The twist-3 DA currents are $J_{3;\pi}^{p,n}(x) = \bar{d}(x) \gamma_5 (iz \cdot \overleftrightarrow{D})^n u(x)$, $J_{3;\pi}^{\sigma,n}(x) = \bar{d}(x) \sigma_{\mu\nu} \gamma_5 (iz \cdot \overleftrightarrow{D})^{n+1} u(x)$ and $J_5^{0\dagger}(0) = \bar{u}(0) \gamma_5 d(0)$. The correction functions can also be translated into

$$\begin{aligned} \Pi_{2;\pi}(p, q) &= (z \cdot q)^{n+2} I_{2;\pi}^{(n,0)}(q^2), \\ \Pi_{3;\pi}^p(p, q) &= (z \cdot q)^n I_{3;\pi}^{p,(n,0)}(q^2), \\ \Pi_{3;\pi}^\sigma(p, q) &= -i(q_\mu z_\nu - q_\nu z_\mu) (z \cdot q)^n I_{3;\pi}^{\sigma,(n,0)}(q^2). \end{aligned} \quad (23)$$

After adopt the traditional QCD sum rule approach, we can get the following analytical expressions for the ξ -moments for twist-2 and twist-3 pion DAs.

$$\begin{aligned} \frac{\langle \xi_{2;\pi}^n \rangle|_\mu \langle \xi_{2;\pi}^0 \rangle|_\mu f_\pi^2}{M^2 e^{m_\pi^2/M^2}} &= \frac{3}{4\pi^2(n+1)(n+3)} \left(1 - e^{-s_{2;\pi}/M^2} \right) + \frac{(m_d + m_u) \langle \bar{q}q \rangle}{(M^2)^2} + \frac{\langle \alpha_s G^2 \rangle}{(M^2)^2} \frac{1 + n\theta(n-2)}{12\pi(n+1)} \\ &- \frac{(m_d + m_u) \langle g_s \bar{q} \sigma T G q \rangle}{(M^2)^3} \frac{8n+1}{18} + \frac{\langle g_s \bar{q}q \rangle^2}{(M^2)^3} \frac{4(2n+1)}{81} - \frac{\langle g_s^3 f G^3 \rangle}{(M^2)^3} \frac{n\theta(n-2)}{48\pi^2} \\ &+ \frac{\langle g_s^2 \bar{q}q \rangle^2}{(M^2)^3} \frac{2 + \kappa^2}{486\pi^2} \left\{ -2(51n+25) \left(-\ln \frac{M^2}{\mu^2} \right) + 3(17n+35) + \theta(n-2) [2n \right. \end{aligned}$$

$$\times \left(-\ln \frac{M^2}{\mu^2} \right) + \frac{49n^2 + 100n + 56}{n} - 25(2n+1) \left[\psi\left(\frac{n+1}{2}\right) - \psi\left(\frac{n}{2}\right) + \ln 4 \right] \right\}. \quad (24)$$

$$\begin{aligned} \frac{\langle \xi_{3;\pi}^{p,n} \rangle |_\mu \langle \xi_{3;\pi}^{p,0} \rangle |_\mu f_\pi^2 \mu_\pi^2}{M^4 e^{m_\pi^2/M^2}} &= \frac{3}{8\pi^2} \frac{1}{2n+1} \left[1 - \left(1 + \frac{s_{3;\pi}^p}{M^2} \right) e^{-s_{3;\pi}^p/M^2} \right] + \frac{2n-1}{2} \frac{(m_u + m_d) \langle \bar{q}q \rangle}{M^4} \\ &+ \frac{2n+3}{24\pi} \frac{\langle \alpha_s G^2 \rangle}{M^4} + \frac{16\pi}{81} [21 + 8n(n+1)] \frac{\langle \sqrt{\alpha_s} \bar{q}q \rangle^2}{M^6} \end{aligned} \quad (25)$$

$$\begin{aligned} \frac{\langle \xi_{3;\pi}^{\sigma,n} \rangle |_\mu \langle \xi_{3;\pi}^{\sigma,0} \rangle |_\mu f_\pi^2 \mu_\pi^2}{M^4 e^{m_\pi^2/M^2}} &= \frac{3}{2n+1} \left\{ \frac{3}{8\pi^2} \frac{1}{2n+3} \left[1 - \left(1 + \frac{s_{3;\pi}^\sigma}{M^2} \right) e^{-s_{3;\pi}^\sigma/M^2} \right] + \frac{2n+1}{2} \frac{(m_u + m_d) \langle \bar{q}q \rangle}{M^4} \right. \\ &+ \left. \frac{2n+1}{24\pi} \frac{\langle \alpha_s G^2 \rangle}{M^4} + \frac{16\pi}{81} (8n^2 - 2) \frac{\langle \sqrt{\alpha_s} \bar{q}q \rangle^2}{M^6} \right\}, \end{aligned} \quad (26)$$

When taking order 0th order ξ -moment normalized to be 1 directly, which is been adopted by many QCD sum rule, there will have extra deviation to predicted $\langle \xi_{2;\pi}^n \rangle |_\mu$ and $\langle \xi_{3;\pi}^{(p,\sigma),n} \rangle |_\mu$. Thus we keep the $\langle \xi_{2;\pi}^0 \rangle |_\mu$ and $\langle \xi_{3;\pi}^{(p,\sigma),0} \rangle |_\mu$ in Eqs. (24)-(26). The detailed derivation for Eq. (24) and Eqs. (25, 26) can be seen in Ref. [68] and Ref. [72], respectively.

III. NUMERICAL ANALYSIS

In order to perform the phenomenological analysis, the following input parameters need to be taken. The pole mass of c -quark is $m_c = 1.50 \pm 0.05$ GeV [74]. The initial and final meson masses are $m_D = 1869.66$ MeV and $m_\pi = 139.57039 \pm 0.00017$ MeV, while the pion decay constant $f_\pi = 130.2 \pm 1.2$ MeV are taken from Particle Data Group (PDG) [75]. The D -meson decay constants are taken as $f_D = 0.163_{-0.021}^{+0.017}$ GeV. The values of non-perturbative vacuum condensates up to six-dimension are taken as follows [76–78],

$$\begin{aligned} \langle \alpha_s G^2 \rangle &= 0.038 \pm 0.011 \text{ GeV}^4, \\ \langle g_s^3 f G^3 \rangle &= 0.045 \pm 0.007 \text{ GeV}^6, \\ \langle g_s \bar{q}q \rangle^2 &= (2.082_{-0.697}^{+0.734}) \times 10^{-3} \text{ GeV}^6, \\ \langle g_s^2 \bar{q}q \rangle^2 &= (7.420_{-2.483}^{+2.614}) \times 10^{-3} \text{ GeV}^6, \\ \langle \bar{q}q \rangle &= (-2.417_{-0.114}^{+0.227}) \times 10^{-2} \text{ GeV}^3, \\ \sum \langle g_s^2 \bar{q}q \rangle^2 &= (1.891_{-0.633}^{+0.665}) \times 10^{-2} \text{ GeV}^6. \end{aligned} \quad (27)$$

The quark-gluon mixture condensate $\langle g_s \bar{q} \sigma T G q \rangle = m_0^2 \langle \bar{q}q \rangle$ with $m_0^2 = 0.80 \pm 0.02 \text{ GeV}^2$. Due to the $D \rightarrow \pi$ processes typical scale is $\mu_k = (m_D^2 - m_c^2) \sim 1.1$ GeV. The renormalization group equations (RGEs) should be used to running the quark masses and each vacuum condensates appearing in the BFTSR from the initial scale $\mu_0 = 1$ GeV to the typical scale μ_k . In QCD sum rule approach, the continuum threshold s_0 and Borel parameter M^2 are the two important parameters which should be determined strictly. In this paper, we take the following four criteria:

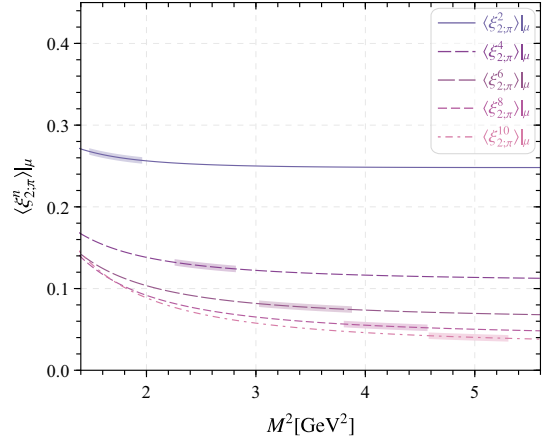


FIG. 1: Moments $\langle \xi_{2;\pi}^n \rangle |_\mu$ up to $n = (2, 4, \dots, 10)$ -order level versus the Borel parameter M^2 . The shaded bands stand for the corresponding Borel windows.

- The continuum contributions are less than 45% of the total results;
- The contributions from the dimension-six condensates do not exceed 5%;
- We require the variations of $\langle \xi_{2;\pi}^n \rangle |_\mu$ within the Borel window to be less than 10%

Based on the above criteria, we determine the value of continuum threshold parameter s_0^π for pion leading-twist DA by using the 0th-order ξ -moments normalization, *i.e.* $\langle \xi_{2;\pi}^0 \rangle |_\mu = 1$. So we have $s_0^\pi = 1.05 \text{ GeV}^2$ for $n = (2, 4, 6, 8, 10)$ -order moments. Furthermore, the allowable region for Borel parameters (also called Borel window) for each order ξ -moments are present in Fig. 1, where the shaded region stand for the Borel windows. From the figure we can see that the Borel window increases with the increase of n th-order, which are all larger than 1. The values of $\langle \xi_{2;\pi}^n \rangle |_\mu$ are decreases with the increase of order n , which can also be seen in our previous work [68]. Then, the first five pion leading-twist DA ξ -moments *i.e.* $\langle \xi_{2;\pi}^n \rangle |_\mu$ with $n = (2, 4, 6, 8, 10)$ combing with the continuum states contributions and

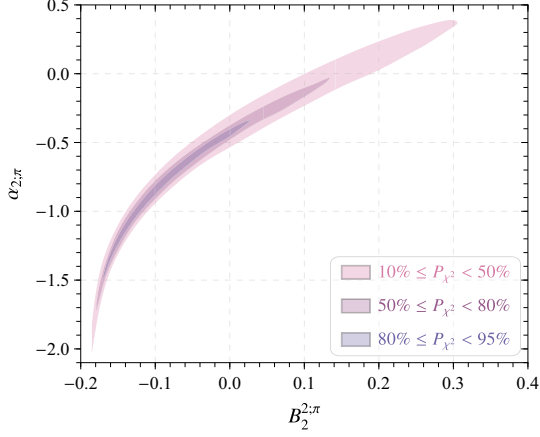


FIG. 2: The relationship curve between parameters $\alpha_{2;\pi}$, $B_2^{2;\pi}$ and goodness of fit $P_{\chi^2_{\min}}$ at factorization scale μ_k .

TABLE I: The ratios of the continuum states' and the dimension-six condensates' contributions over the total moments of π -meson twist-2 LCDA $\langle \xi_{2;\pi}^n \rangle|_\mu$ with $n = (2, 4, 6, 8, 10)$ within the determined Borel windows. The abbreviations "Con." and "Six." stand for the continuum and dimension-six contributions, respectively.

n	Con.	Six.	$\langle \xi_{2;\pi}^n \rangle _\mu$
2	< 35%	< 5%	0.267 ± 0.012
4	< 35%	< 5%	0.135 ± 0.009
6	< 40%	< 5%	0.085 ± 0.008
8	< 40%	< 5%	0.062 ± 0.006
10	< 45%	< 5%	0.048 ± 0.005

dimension-six contributions are listed in Table I. When $n = (2, 4, 6, 8, 10)$, the continuum contributions are set to be less than 35%, 35%, 40%, 40%, 45%, respectively. The dimension-six condensates' contributions to be less than 5% for all the order of $\langle \xi_{2;\pi}^n \rangle|_\mu$.

In Fig. 2, the relationship between fitting parameters $\alpha_{2;\pi}$, $B_2^{2;\pi}$ and the goodness of fit at scale μ_k is plotted. The shaded bands stand for the corresponding Borel windows. The depth of color in the shaded band represents the degree of goodness of fit. The deeper the color, the higher the goodness of fit. When the range of goodness of fit is $80\% \leq P_{\chi^2_{\min}} \leq 96\%$, the effect for goodness of fit is the best. The obtained optimal values of the model parameters $\alpha_{2;\pi}$, $\hat{a}_2^{2;\pi}$ and $\beta_{2;\pi}$ at scale $\mu_0 = 1$ GeV are

$$\begin{aligned} A_{2;\pi} &= 3.659 \text{ GeV}^{-1}, & \alpha_{2;\pi} &= -1.010, \\ \hat{a}_2^{2;\pi} &= -0.126, & \beta_{2;\pi} &= 0.727 \text{ GeV}. \end{aligned} \quad (28)$$

The corresponding behaviors of pion leading-twist DAs $\phi_{2;\pi}(x, \mu_0)$ at initial scale $\mu_0 = 1$ GeV of our LCHO predictions is shown in Fig. 3. As a comparison, the model in literature for π -meson leading-twist DA $\alpha_{2;\pi}$ such as LQCD model [49], DS model [50], QCD/AdS

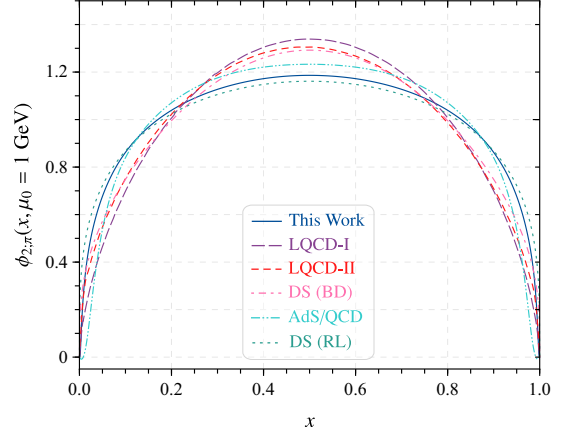


FIG. 3: The pion leading-twist DA curves of our prediction. As a comparison, we also present the LQCD [49], DS model with BD and RL scheme [50] and QCD/AdS model [51] as a comparison.

model [51]. From the Fig. 3, one can find that our present prediction for $\phi_{2;\pi}$ is closely to DS model and QCD/AdS model.

As for the pion twist-3 DA ξ -moments, we take the continuum threshold $s_{3;\pi}^p = s_{3;\pi}^s = 1.69(10) \text{ GeV}^2$ and $\langle \xi_{3;\pi}^{p,0} \rangle|_\mu = 1$. After followed by the traditional criteria in determine the Borel window, we can get the first two order moments, which can be found in our previous work [72]. With the resultant $\langle \xi_{3;\pi}^{(p,\sigma),(2,4)} \rangle|_\mu$, we calculated the wavefunction parameters at initial scale $\mu_0 = 1$ GeV have the following values

$$\begin{aligned} A_{3;\pi}^p &= 78.72 \text{ GeV}^{-2}, & B_{3;\pi}^p &= 0.476, \\ C_{3;\pi}^p &= 0.943, & \beta_{3;\pi}^p &= 0.608 \text{ GeV}, \end{aligned} \quad (29)$$

$$\begin{aligned} A_{3;\pi}^\sigma &= 160.5 \text{ GeV}^{-2}, & B_{3;\pi}^\sigma &= -0.027, \\ C_{3;\pi}^\sigma &= 0.933, & \beta_{3;\pi}^\sigma &= 0.424 \text{ GeV}. \end{aligned} \quad (30)$$

The corresponding behaviors of pion twist-3 DAs $\phi_{2;\pi}$ of our LCHO predictions is shown in Fig. 4. As a comparison, we also present other QCDSR results from literature for π -meson twist-3 DAs are also present, which is labeled as QCDSR-I [47] and QCDSR-II [55]. Different with twist-2 DA, the pion twist-3 DAs especially for the $\phi_{3;\pi}^p(x)$ have larer discrepancy with other theoretical predictions. As can be seen in the upper panel of Fig. 4, our predictions have agreement with the QCDSR-II in the middle x -region, *i.e.* $0.3 \leq x \leq 0.7$, but have large difference in the region $0 \leq x < 0.3$ and $0.7 < x \leq 1$. For the $\phi_{3;\pi}^\sigma(x)$, the curve of our prediction have the same tendency with QCDSR-I. As for the twist-4 DAs, we take the expressions and input parameters from Ref. [60].

Based on the resultant pion twist-2 and 3 DA, we can then calculate the $D \rightarrow \pi$ TFFs $f_+^{D \rightarrow \pi}(q^2)$ and

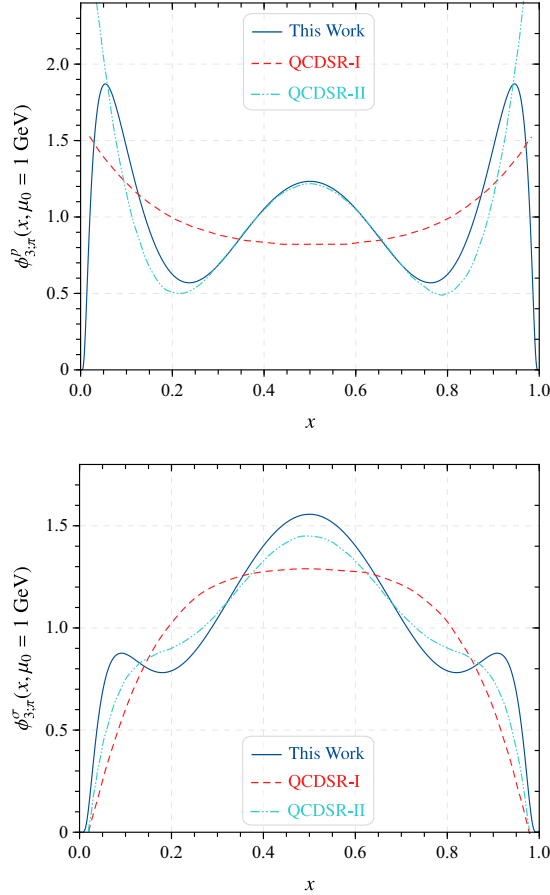


FIG. 4: The pion twist-3 DAs $\phi_{3;\pi}^p(x, \mu_0)$ and $\phi_{3;\pi}^\sigma(x, \mu_0)$ in this work. Meanwhile, predictions coming from QCDSR-I [47], and QCDSR-II [55] are also given as a comparison.

$f_0^{D \rightarrow \pi}(q^2)$. The basic input parameters have been mentioned in the beginning of this section. So the main task is to determine the continuum threshold parameter s_0 and Borel windows M^2 . Based on the basic ideas and processes of LCSR, we adopt the following three criteria.

- The continuum contributions are less than 30% to

TABLE II: Comparison of theoretical predictions for the form factors $f_+^{D \rightarrow \pi}(0)$.

References	$f_+^{D \rightarrow \pi}(0)$
This work	$0.627^{+0.120}_{-0.080}$
Belle [39]	$0.624 \pm 0.020 \pm 0.030$
BESIII [40]	$0.637 \pm 0.008 \pm 0.004$
BES [79]	$0.730 \pm 0.14 \pm 0.0060$
BaBar [41]	$0.610 \pm 0.020 \pm 0.005$
CLEO [42]	$0.640 \pm 0.03 \pm 0.06$
LQCD [43]	$0.640 \pm 0.03 \pm 0.06$
LCSR [80]	0.630 ± 0.110

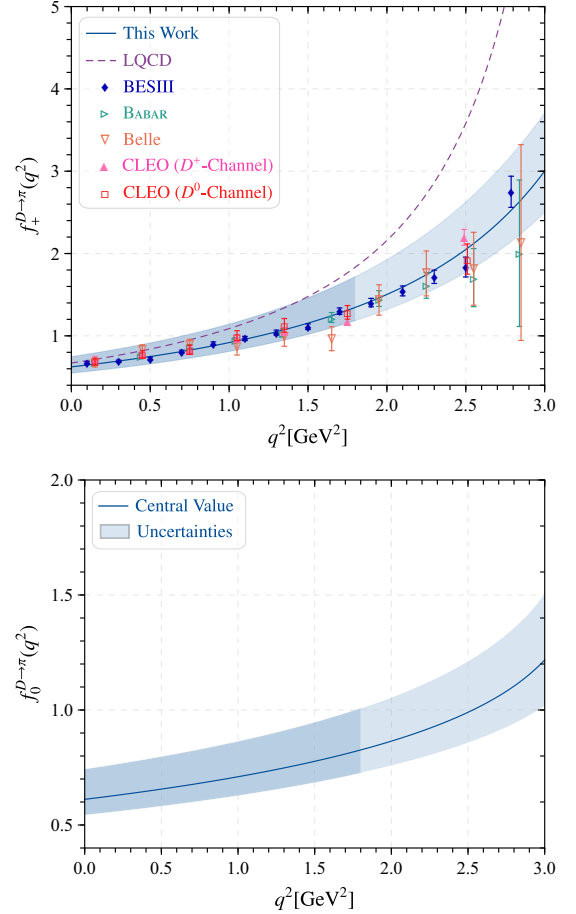


FIG. 5: $D \rightarrow \pi$ TFFs $f_+^{D \rightarrow \pi}(q^2)$ and $f_0^{D \rightarrow \pi}(q^2)$ in the whole physical region within uncertainties in this work. The results of other theoretical and experimental groups such as Belle [39], BESIII [40], BaBar [41], CLEO [42] and LQCD [43] collaborations are also shown as a comparison.

the total results;

- The contributions from higher-twist DAs are less than 5%;
- Within the Borel window, the changes of TFFs does not exceed 10%
- The continuum threshold s_0 should be closer to the squared mass of the first excited state D -meson.

So, we determined the continuum threshold parameter are $s_0^+ = \tilde{s}_0 = 5.2(3) \text{ GeV}^2$. The Borel parameters are $M_+^2 = 8.0(5) \text{ GeV}^2$ and $\tilde{M}^2 = 10.0(5) \text{ GeV}^2$. After considering the errors coming from all the input parameters, we present the TFFs at large recoil region, *e. g.* $f_+^{D \rightarrow \pi}(0) = f_0^{D \rightarrow \pi}(0)$ in Table II. In which, the uncertainties are from the squared average of all the mentioned error sources. As a comparison, we also present other theoretical and experimental predictions, such as the Belle [39], BESIII [40], BES [79], BABAR [41],

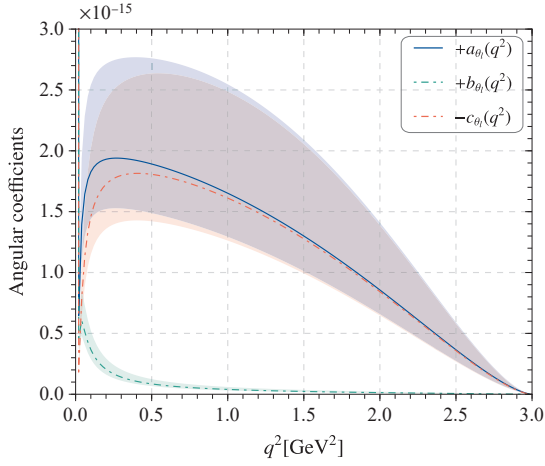


FIG. 6: The distribution of three q^2 -dependent angular coefficient functions $a_{\theta_\ell}(q^2)$, $b_{\theta_\ell}(q^2)$ and $c_{\theta_\ell}(q^2)$ (in unit: 10^{-15}), where the shaded bands stand for the uncertainties.

CLEO [42] Collaborations for the experimental predictions, LQCD [43], LCSR [80] for the theoretical predictions respectively. Our results agree well with the BESIII, Belle, LQCD, BABAR, LCSR and CLEO predictions within errors.

The physically allowable ranges for the $D \rightarrow \pi$ TFFs are $0 \leq q^2 \leq q_{\max}^2 = (m_D - m_\pi)^2 \sim 3 \text{ GeV}^2$. Theoretically, the LCSRs approach for $D \rightarrow \pi \nu \bar{\nu}$ TFFs are in low and intermediate q^2 -regions, i.e. $0 \leq q^2 \leq 1.8 \text{ GeV}^2$ of π -meson. One can extrapolate it to whole q^2 -regions via a rapidly $z(q^2, t)$ converging the simplified series expansion (SSE), i.e. the TFFs are expand as [81]:

$$f_+^{D \rightarrow \pi}(q^2) = \frac{1}{1 - q^2/m_D^2} \sum_{k=0,1,2} \beta_k z^k(q^2, t_0) \quad (31)$$

where β_k are real coefficients and $z(q^2, t)$ is the function,

$$z^k(q^2, t_0) = \frac{\sqrt{t_+ - q^2} - \sqrt{t_+ - t_0}}{\sqrt{t_+ - q^2} + \sqrt{t_+ - t_0}}, \quad (32)$$

with $t_\pm = (m_D \pm m_\pi)^2$ and $t_0 = t_\pm(1 - \sqrt{1 - t_-/t_+})$. The SSE method possesses superior merit, which keeps the analytic structure correct in the complex plane and ensures the appropriate scaling, $f_+^{D \rightarrow \pi}(q^2) \sim 1/q^2$ at large q^2 . And the quality of fit Δ is devoted to take stock of the resultant of extrapolation, which is defined as

$$\Delta = \frac{\sum_t |F_i(t) - F_i^{\text{fit}}(t)|}{\sum_t |F_i(t)|} \times 100. \quad (33)$$

After making extrapolation for the TFFs $f_+^{D \rightarrow \pi}(q^2)$ to the whole physical q^2 -region. Then, the behaviors of $D \rightarrow \pi$ TFFs in the whole physical region with respect to squared momentum transfer are given in Fig. 5. In which, the darker band are the LCSR results of our prediction,

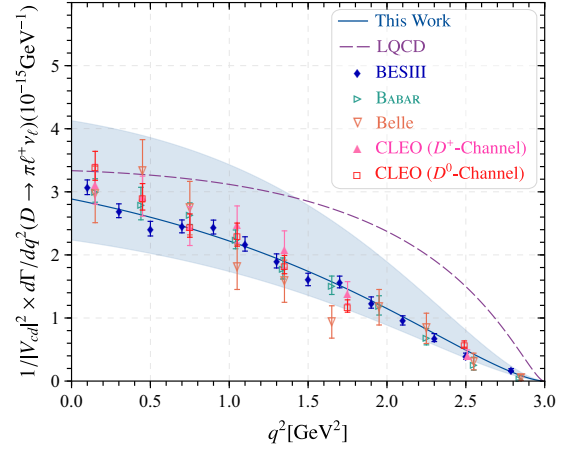


FIG. 7: The predictions of our calculation for $D \rightarrow \pi \ell^+ \nu_\ell$ differential decay width within uncertainties (in unit: 10^{-15}). Meanwhile, the results of other experimental groups such as Belle [39], BESIII [40] BABAR [41], CLEO [42] Collaborations and LQCD prediction [43] are also presented as a comparison.

while the lighter band are the SSE predictions. As a comparison, we also present the predictions from theoretical and experimental groups, such as the LQCD [43], Belle [39], BABAR [41], CLEO [42] and BESIII [40] collaborations are also presented. Our predictions have a good agreement with the experimental collaborations within errors. We found at the large squared momentum transfer, the predictions from LQCD have large gap with our results. Meanwhile, we also present the TFF $f_0^{D \rightarrow \pi}(q^2)$ in the lower panel of Fig. 5. Furthermore, we present the behaviors of three angular coefficients functions $a_{\theta_\ell}(q^2)$, $b_{\theta_\ell}(q^2)$ and $c_{\theta_\ell}(q^2)$ uncertainties with 10^{-17} -order level in Fig. 6. The negative of c_{θ_ℓ} is given for convenience to compare the three angular coefficients. As can be seen from the figure, the absolute values of $a_{\theta_\ell}(q^2)$ and $c_{\theta_\ell}(q^2)$ are very closer with uncertainties, and value for $b_{\theta_\ell}(q^2)$ is smaller than that of $a_{\theta_\ell}(q^2)$ and $-c_{\theta_\ell}(q^2)$.

Then our task is to calculate the decay width and branching fraction for the semileptonic decay processes $\bar{D}^0 \rightarrow \pi^+ e \bar{\nu}_e$. By taking the $D \rightarrow \pi$ TFFs $f_{+,0}^{D \rightarrow \pi}(q^2)$ or angular coefficient function $a_{\theta_\ell}(q^2)$, $b_{\theta_\ell}(q^2)$, $c_{\theta_\ell}(q^2)$ into the expression of decay width, e.g. Eq. (5), we present the curves of $D^+ \rightarrow \pi e \nu_e$ differential decay width in Fig. 7 (in unit: 10^{-15}) with darker band are the uncertainties coming from all the input parameters. As a comparison, we also listed the predictions from Belle [39], BESIII [40] BABAR [41], CLEO [42] Collaborations and LQCD prediction [43] as a comparison. From the figure, we can see that the results of our predictions have agreement with the most experimental results within uncertainties, especially for the BESIII Collaboration.

Furthermore, after considering the D^0 -meson lifetime $\tau(D^0) = 0.410(1) \text{ ps}$ coming from PDG [75] and integrate the squared momentum transfer q^2 , we can get the

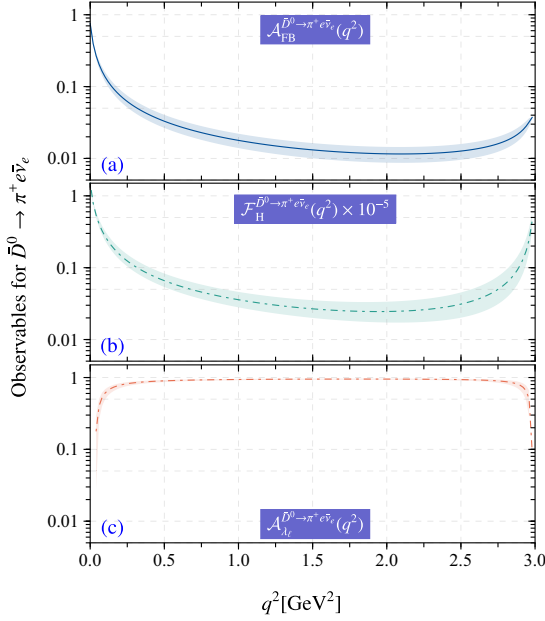


FIG. 8: Theory prediction for the three various items angular observables $\mathcal{A}_{\text{FB}}^{\bar{D}^0 \rightarrow \pi^+ e \bar{\nu}_e}(q^2)$, $\mathcal{F}_{\text{H}}^{\bar{D}^0 \rightarrow \pi^+ e \bar{\nu}_e}(q^2)$, and $\mathcal{A}_{\lambda_\ell}^{\bar{D}^0 \rightarrow \pi^+ e \bar{\nu}_e}(q^2)$. In which, the shaded bands stand for uncertainties.

value of total branching fraction for the $D^0 \rightarrow \pi^- e^+ \nu_e$, which are shown in Table III. The error of our prediction are comes from all input parameters. To make a comparison, we also present the PDG [56], Belle [39], BESIII [40], BES [79], BABAR [41], CLEO [42] and LQCD [43] predictions. The value of our prediction have agreement with BESIII, PDG average value and LQCD results.

On the other hand, the observables such as forward-backward asymmetries, q^2 -differential flat terms and lepton polarization asymmetry, *e.g.* $\mathcal{A}_{\text{FB}}^{\bar{D}^0 \rightarrow \pi^+ e \bar{\nu}_e}(q^2)$, $\mathcal{F}_{\text{H}}^{\bar{D}^0 \rightarrow \pi^+ e \bar{\nu}_e}(q^2)$ and $\mathcal{A}_{\lambda_\ell}^{\bar{D}^0 \rightarrow \pi^+ e \bar{\nu}_e}(q^2)$ can be obtained by using the resultant three angular coefficient, which can be found in our previous work [82]. The normalized forward-backward asymmetries and q^2 differential flat terms will

TABLE III: The branching fraction (in unit 10^{-2}) for semileptonic decay $\bar{D}^0 \rightarrow \pi^+ e \bar{\nu}_e$ of our predictions. Meanwhile, the theoretical and experimental results from other group are also given as a comparison.

References	Channel	Predictions
This work	$\bar{D}^0 \rightarrow \pi^+ e \bar{\nu}_e$	$0.308^{+0.155}_{-0.066}$
PDG [56]	$\bar{D}^0 \rightarrow \pi^+ e \bar{\nu}_e$	0.281 ± 0.190
Belle [39]	$D^0 \rightarrow \pi^- \ell^+ \nu_\ell$	$0.255 \pm 0.019 \pm 0.016$
BESIII [40]	$D^0 \rightarrow \pi^- e^+ \nu_e$	$0.295 \pm 0.004 \pm 0.003$
BES [79]	$D^0 \rightarrow \pi^- e^+ \nu_e$	$0.330 \pm 0.130 \pm 0.030$
BaBar [41]	$D^0 \rightarrow \pi^- e^+ \nu_e$	$0.277 \pm 0.068 \pm 0.0092 \pm 0.037$
CLEO [42]	$D^0 \rightarrow \pi^- e^+ \nu_e$	$0.288 \pm 0.008 \pm 0.003$
LQCD [43]	$D^0 \rightarrow \pi^- \ell^+ \nu_\ell$	$0.316 \pm 0.025 \pm 0.062 \pm 0.033$

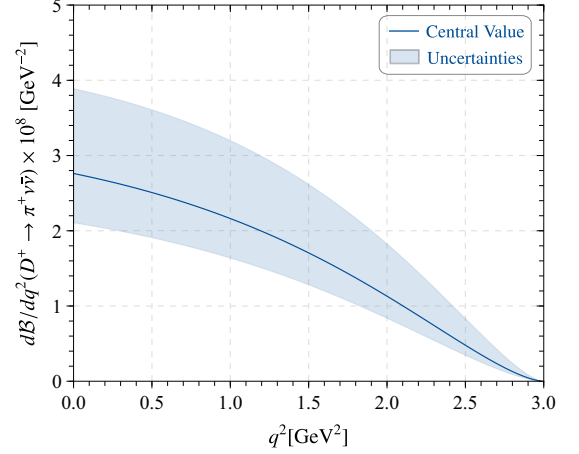


FIG. 9: The predictions of our calculation for $D^+ \rightarrow \pi^+ \nu \bar{\nu}$ differential decay width within uncertainties (in unit: 10^{-8}). Meanwhile, which is consistent with the upper limit of the experimental prediction results of BESIII [40] collaborations.

vanish in the massless lepton limit to the SM, which is sensitive to beyond standard model (BSM). Meanwhile, the lepton polarization asymmetry is sensitive to helicity-violating new physics interactions. So, we display the three curves in Fig. 8 with (a), (b) and (c) panel respectively. The q^2 differential flat terms is in unit 10^{-5} order. The uncertainties of lepton polarization is very small that almost coincidence with central value. For the next step, we can calculate the rare FCNC decays $D^+ \rightarrow \pi^+ \nu \bar{\nu}$. The input parameters are: Weinberg angle $\sin^2 \theta_W = 0.2312$, electromagnetic coupling constant α_{em} , running coupling constant $\alpha_s(1.1\text{GeV}) = 0.4256$, Fermi constant $G_F = 1.166 \times 10^{-5} \text{GeV}^{-2}$ and $C_F = 4/3$. The curve for differential branching fraction of $D^+ \rightarrow \pi^+ \nu \bar{\nu}$ within uncertainties are exhibit in Fig. 9. Due to other theoretical predictions such as Ref. [56] is in 10^{-7} order, we do not show here to make a comparison.

Then, we present the branching ratio of dineutrino decay mode $D \rightarrow \pi \nu \bar{\nu}$ in Table IV within uncertainties. The NSI [8], the SM with Long Distance and short distance [83], the LU, cLFC and General from Ref. [84] are also given. As can be seen that our prediction is in the same order with NSIs prediction, larger than the SM and lower than the LU, cLFC, General results. Meanwhile, our prediction also have the same order with BESIII result.

IV. SUMMARY

In the paper, the rate decay process of $D^+ \rightarrow \pi^+ \nu \bar{\nu}$ is studied within the framework of QCD sum rule approach. Firstly, we give expression of pion twist-2 and twist-3 DAs $\xi_{2;\pi}^n|_\mu$ and $\langle \xi_{3;\pi}^{(p,\sigma),n} \rangle|_\mu$ by us-

TABLE IV: The $D^+ \rightarrow \pi^+ \nu \bar{\nu}$ branching fraction in this work. Meanwhile, the theoretical and experimental results are given with comparison.

References	Result
This Work	$1.85^{+0.93}_{-0.46} \times 10^{-8}$
NSIs [8]	3.21×10^{-8}
SM [83] (Long Distance)	$< 8 \times 10^{-16}$
SM [83] (Short Distance)	3.9×10^{-16}
LU [84]	$< 2.5 \times 10^{-6}$
cLFC [84]	$< 1.4 \times 10^{-5}$
General [84]	$< 5.2 \times 10^{-5}$

ing the QCD sum rule approach under the background field theory. The first five terms to the twist-2 DA and first two terms of the ξ -moments are given in the processes scale $\mu_k = 1.1$ GeV. In order to avoid the large uncertainties coming from Gegenbauer moment a_n , we constructed the LCHO model for twist-2, 3 LCDAs and determined the parameters by using the ξ -moments.

Secondly, we calculated the $D \rightarrow \pi$ vector and scalar TFFs within the QCD light-cone sum rule approach up to next-to-leading order accuracy. The value of TFF at large recoil region $f_+^{D \rightarrow \pi}(0)$ is present in Table II. After extrapolate the TFFs into whole q^2 -region via simplified series expansion, we give the TFFs in Fig. 5. The comparison with other predictions is made. Meanwhile, the

three q^2 -dependence angular coefficient functions $a_{\theta_\ell}(q^2)$, $b_{\theta_\ell}(q^2)$ and $c_{\theta_\ell}(q^2)$ are also given.

Furthermore, we analysis the differential decay width for $D^+ \rightarrow \pi^+ e \nu_e$ in Fig. 7 and make a detailed comparison with BESIII, BABAR, Belle, CLEO and LQCD predictions. The total branching fraction for $\bar{D}^0 \rightarrow \pi^+ e \bar{\nu}_e$ is given in Table III. Then we give the forward-backward asymmetries, q^2 differential flat terms, lepton polarization asymmetry in Fig. 8. Finally, the differential and total branching fraction of $D^+ \rightarrow \pi^+ \nu \bar{\nu}$ are given in Fig. 9 and Table IV. Our prediction is in the region of the BESIII upper limits. With the stable operation of BESIII, the collision energy of BEPC-II collider will be greatly improved in the following seven years and more data results will be reported. We hope the $D^+ \rightarrow \pi^+ \nu \bar{\nu}$ channel prediction can be reported in the near further.

Acknowledgments

This work was supported in part by the National Natural Science Foundation of China under Grant No.12265010, No.12265009, the Project of Guizhou Provincial Department of Science and Technology under Grant No.ZK[2021]024 and No.ZK[2023]142.

-
- [1] G. Burdman, E. Golowich, J. L. Hewett and S. Pakvasa, Rare charm decays in the standard model and beyond, *Phys. Rev. D* **66** (2002) 014009. [[hep-ph/0112235](#)]
 - [2] S. L. Glashow, J. Iliopoulos and L. Maiani, Weak Interactions with Lepton-Hadron Symmetry, *Phys. Rev. D* **2** (1970) 1285-1292.
 - [3] D. M. Asner, T. Barnes, J. M. Bian, I. I. Bigi, N. Brambilla, I. R. Boyko, V. Bytev, K. T. Chao, J. Charles and H. X. Chen, *et al.* Physics at BES-III, *Int. J. Mod. Phys. A* **24** (2009) S1-794. [[arXiv:0809.1869](#)]
 - [4] M. Saur and F. S. Yu, Charm CPV: observation and prospects, *Sci. Bull.* **65** (2020), 1428-1431. [[arXiv:2002.12088](#)].
 - [5] G. Wilkinson, Charming synergies: the role of charm-threshold studies in the search for physics beyond the Standard Model, *Sci. Bull.* **66** (2021) 2251. [[arXiv:2107.08414](#)]
 - [6] L. Cappiello, O. Cata and G. D'Ambrosio, Standard Model prediction and new physics tests for $D^0 \rightarrow h^+ h^- \ell^+ \ell^-$ ($h = \pi, K$; $\ell = e, \mu$), *JHEP* **04** (2013) 135. [[arXiv:1209.4235](#)]
 - [7] R. Aaij *et al.* [LHCb Collaboration], Observation of D^0 meson decays to $\pi^+ \pi^- \mu^+ \mu^-$ and $K^+ K^- \mu^+ \mu^-$ final states, *Phys. Rev. Lett.* **119** (2017) 181805. [[arXiv:1707.08377](#)]
 - [8] S. Mahmood, F. Tahir and A. Mir, A search of new physics with $D_s^+ \rightarrow D^+ \nu \bar{\nu}, B_s^0 \rightarrow B^0 \nu \bar{\nu}, K^+ \rightarrow \pi^+ \nu \bar{\nu}, D^+ \rightarrow \pi^+ \nu \bar{\nu}, D^0 \rightarrow \pi^0 \nu \bar{\nu}$ and $D_s^+ \rightarrow K^+ \bar{\nu}$, *Int. J. Mod. Phys. E* **24** (2015) 1571001. [[arXiv:1411.2430](#)]
 - [9] I. I. Bigi and A. Paul, On CP Asymmetries in Two-, Three- and Four-Body D Decays, *JHEP* **03** (2012) 021. [[arXiv:1110.2862](#)]
 - [10] R. Bause, H. Gisbert, M. Golz and G. Hiller, Rare charm $c \rightarrow u \nu \bar{\nu}$ dineutrino null tests for $e^+ e^-$ machines, *Phys. Rev. D* **103** (2021) 015033. [[arXiv:2010.02225](#)]
 - [11] R. Aaij *et al.* [LHCb Collaboration], Test of lepton universality in beauty-quark decays, *Nature Phys.* **18** (2022) 277-282. [[arXiv:2103.11769](#)]
 - [12] R. K. Ellis, B. Heinemann, J. de Blas, M. Cepeda, C. Grojean, F. Maltoni, A. Nisati, E. Petit, R. Rattazzi and W. Verkerke, *et al.* Physics Briefing Book: Input for the European Strategy for Particle Physics Update 2020, [[arXiv:1910.11775](#)]
 - [13] M. Ablikim *et al.* [BESIII Collaboration], Search for the decay $D^0 \rightarrow \pi^0 \nu \bar{\nu}$, *Phys. Rev. D* **105** (2022) L071102. [[arXiv:2112.14236](#)]
 - [14] F. J. Botella, C. S. Lim and W. J. Marciano, Radiative Corrections to Neutrino Indices of Refraction, *Phys. Rev. D* **35** (1987), 896.
 - [15] J. W. F. Valle, Resonant Oscillations of Massless Neutrinos in Matter, *Phys. Lett. B* **199** (1987) 432-436.
 - [16] E. Roulet, MSW effect with flavor changing neutrino interactions, *Phys. Rev. D* **44** (1991) R935-R938.
 - [17] M. M. Guzzo, A. Masiero and S. T. Petcov, On the MSW effect with massless neutrinos and no mixing in the vacuum, *Phys. Lett. B* **260** (1991) 154-160.
 - [18] S. Bergmann, M. M. Guzzo, P. C. de Holanda,

- P. I. Krastev, and H. Nunokawa, Status of the solution to the solar neutrino problem based on non-standard neutrino interactions, *Phys. Rev. D* **62** (2000) 073001. [[hep-ph/0004049](#)]
- [19] M. M. Guzzo, H. Nunokawa, P. C. de Holanda, and O. L. G. Peres, On the massless ‘just-so’ solution to the solar neutrino problem, *Phys. Rev. D* **64**, 097301 (2001). [[hep-ph/0012089](#)]
- [20] M. Guzzo, P. C. de Holanda, M. Maltoni, H. Nunokawa, M. A. Tortola, and J. W. F. Valle, Status of a hybrid three-neutrino interpretation of neutrino data, *Nucl. Phys. B* **629** (2002) 479. [[hep-ph/0112310](#)]
- [21] Y. Grossman, Non-standard Neutrino Interactions And Neutrino Oscillation Experiments, *Phys. Lett. B* **359** (1995) 141. [[hep-ph/9507344](#)];
- [22] S. Bergmann, Y. Grossman, and E. Nardi, Neutrino propagation in matter with general interactions, *Phys. Rev. D* **60** (1999) 093008. [[hep-ph/9903517](#)]
- [23] A. De Gouvea, G. F. Giudice, A. Strumia and K. Tobe, Phenomenological implications of neutrinos in extra dimensions, *Nucl. Phys. B* **623** (2002) 395-420. [[hep-ph/0107156](#)]
- [24] S. Davidson, C. Pena-Garay, N. Rius and A. Santamaria, Present and future bounds on nonstandard neutrino interactions, *JHEP* **03** (2003) 011. [[hep-ph/0302093](#)]
- [25] L. M. Johnson and D. W. McKay, Revising neutrino oscillation parameter space with direct flavor changing interactions, *Phys. Rev. D* **61** (2000) 113007. [[hep-ph/9909355](#)]
- [26] A. M. Gago, M. M. Guzzo, H. Nunokawa, W. J. C. Teves and R. Zukanovich Funchal, Probing flavor changing neutrino interactions using neutrino beams from a muon storage ring, *Phys. Rev. D* **64** (2001) 073003. [[hep-ph/0105196](#)]
- [27] T. Ota and J. Sato, Can ICARUS and OPERA give information on a new physics? *Phys. Lett. B* **545** (2002) 367-372. [[hep-ph/0202145](#)]
- [28] T. Ota, J. Sato, and N. Yamashita, Oscillation enhanced search for new interaction with neutrinos, *Phys. Rev. D* **65** (2002) 093015. [[hep-ph/0112329](#)]
- [29] M. Campanelli and A. Romanino, Effects of new physics in neutrino oscillations in matter, *Phys. Rev. D* **66** (2002) 113001. [[hep-ph/0207350](#)]
- [30] P. Huber, T. Schwetz, and J. W. F. Valle, How sensitive is a neutrino factory to the angle θ_{13} ? *Phys. Rev. Lett.* **88** (2002) 101804. [[hep-ph/0111224](#)]
- [31] N. Kitazawa, H. Sugiyama and O. Yasuda, Will MINOS see new physics? [hep-ph/0606013](#).
- [32] V. D. Barger, R. J. N. Phillips, and K. Whisnant, Solar neutrino solutions with matter enhanced flavor changing neutral current scattering, *Phys. Rev. D* **44** (1991) 1629.
- [33] Z. Berezhiani and A. Rossi, Limits on the non-standard interactions of neutrinos from e^+e^- colliders, *Phys. Lett. B* **535** (2002) 207. [[hep-ph/0111137](#)]
- [34] J. Barranco, O. G. Miranda, C. A. Moura, and J. W. F. Valle, Constraining non-standard interactions in $\nu_e e$ or $\bar{\nu}_e e$ scattering, *Phys. Rev. D* **73** (2006) 113001. [[hep-ph/0512195](#)]
- [35] G. Mangano, G. Miele, S. Pastor, T. Pinto, O. Pisanti, and P. D. Serpico, Effects of non-standard neutrino electron interactions on relic neutrino decoupling, *Nucl. Phys. B* **756** (2006) 100. [[hep-ph/0607267](#)]
- [36] M. Blennow, T. Ohlsson, and J. Skrotzki, Effects of non-standard interactions in the MINOS experiment, *Phys. Lett. B* **660** (2008) 522-528. [[hep-ph/0702059](#)];
- [37] J. Barranco, O. G. Miranda, and T. I. Rashba, Low energy neutrino experiments sensitivity to physics beyond the standard model, *Phys. Rev. D* **76** (2007) 073008. [[hep-ph/0702175](#)];
- [38] J. Kopp, M. Lindner, and T. Ota, Discovery reach for non-standard interactions in a neutrino factory, *Phys. Rev. D* **76** (2007) 013001. [[hep-ph/0702269](#)]
- [39] L. Widhalm *et al.* [Belle Collaboration], Measurement of $D^0 \rightarrow \pi l \nu (K l \nu)$ Form Factors and Absolute Branching Fractions, *Phys. Rev. Lett.* **97** (2006) 061804. [[hep-ex/0604049](#)]
- [40] M. Ablikim *et al.* [BESIII Collaboration], Study of Dynamics of $D^0 \rightarrow K^- e^+ \nu_e$ and $D^0 \rightarrow \pi^- e^+ \nu_e$ Decays, *Phys. Rev. D* **92** (2015) 072012. [[arXiv:1508.07560](#)]
- [41] J. P. Lees *et al.* [BaBar Collaboration], Measurement of the $D^0 \rightarrow \pi^- e^+ \nu_e$ differential decay branching fraction as a function of q^2 and study of form factor parameterizations, *Phys. Rev. D* **91** (2015) 052022. [[arXiv:1412.5502](#)]
- [42] D. Besson *et al.* [CLEO Collaboration], Improved measurements of D meson semileptonic decays to π and K mesons, *Phys. Rev. D* **80** (2009) 032005. [[arXiv:0906.2983](#)]
- [43] C. Aubin *et al.* [Fermilab Lattice, MILC and HPQCD], Semileptonic decays of D mesons in three-flavor lattice QCD, *Phys. Rev. Lett.* **94** (2005) 011601. [[hep-ph/0408306](#)]
- [44] A. Khodjamirian, R. Ruckl, S. Weinzierl, C. W. Winhart and O. I. Yakovlev, Predictions on $B \rightarrow \pi \ell \nu_\ell$, $D \rightarrow \pi \ell \nu_\ell$ and $D \rightarrow K \ell \nu_\ell$ from QCD light cone sum rules, *Phys. Rev. D* **62** (2000) 114002. [[hep-ph/0001297](#)]
- [45] R. C. Verma, Decay constants and form factors of s-wave and p-wave mesons in the covariant light-front quark model, *J. Phys. G* **39** (2012) 025005. [[arXiv:1103.2973](#)]
- [46] S. Fajfer and J. F. Kamenik, Charm meson resonances in $D \rightarrow P \ell \nu$ decays, *Phys. Rev. D* **71** (2005) 014020. [[hep-ph/0412140](#)]
- [47] P. Ball, Theoretical update of pseudoscalar meson distribution amplitudes of higher twist: The Nonsinglet case, *JHEP* **01** (1999) 010. [[hep-ph/9812375](#)]
- [48] P. Ball, V. M. Braun and A. Lenz, Higher-twist distribution amplitudes of the K meson in QCD, *JHEP* **05** (2006) 004. [[hep-ph/0603063](#)]
- [49] G. S. Bali *et al.* [RQCD Collaboration], Light-cone distribution amplitudes of pseudoscalar mesons from lattice QCD, *JHEP* **1908** (2019) 065. [[arXiv:1903.08038](#)]
- [50] L. Chang, I. C. Cloet, J. J. Cobos-Martinez, C. D. Roberts, S. M. Schmidt and P. C. Tandy, Imaging dynamical chiral symmetry breaking: pion wave function on the light front, *Phys. Rev. Lett.* **110** (2013) 132001. [[arXiv:1301.0324](#)]
- [51] M. Ahmady, C. Mondal and R. Sandapen, Dynamical spin effects in the holographic light-front wavefunctions of light pseudoscalar mesons, *Phys. Rev. D* **98** (2018) 034010. [[arXiv:1805.08911](#)]
- [52] A. J. Arifi, H. M. Choi and C. R. Ji, Pseudoscalar meson decay constants and distribution amplitudes up to the twist-4 in the light-front quark model, *Phys. Rev. D* **108** (2023) 013006. [[arXiv:2306.08536](#)]
- [53] T. Huang, X. H. Wu and M. Z. Zhou, Twist three distribute amplitudes of the pion in QCD sum rules, *Phys. Rev. D* **70** (2004) 014013. [[hep-ph/0402100](#)]
- [54] T. Huang, M. Z. Zhou and X. H. Wu, Twist-3 distribution amplitudes of the pion and kaon from the QCD sum

- rules, *Eur. Phys. J. C* **42** (2005) 271. [[hep-ph/0501032](#)]
- [55] V. M. Braun and I. E. Filyanov, Conformal Invariance and Pion Wave Functions of Nonleading Twist, *Z. Phys. C* **48** (1990) 239-248.
- [56] C. H. Chen, C. Q. Geng and T. C. Yuan, Non-standard neutrino interactions in $K^+ \rightarrow \pi^+ \nu \bar{\nu}$ and $D^+ \rightarrow \pi^+ \nu \bar{\nu}$ decays, *Phys. Rev. D* **75** (2007) 077301. [[hep-ph/0703196](#)]
- [57] D. Becirevic, S. Fajfer, I. Nisandzic and A. Tayduganov, Angular distributions of $B \rightarrow D^{(*)} \ell \bar{\nu}_\ell$ decays and search of New Physics, *Nucl. Phys. B* **946** (2019) 114707. [[arXiv:1602.03030](#)]
- [58] B. Y. Cui, Y. K. Huang, Y. L. Shen, C. Wang and Y. M. Wang, Precision calculations of $B_{d,s} \rightarrow \pi, K$ decay form factors in soft-collinear effective theory, *JHEP* **03** (2023) 140. [[arXiv:2212.11624](#)]
- [59] A. Khodjamirian, C. Klein, T. Mannel and N. Offen, Semileptonic charm decays $D \rightarrow \pi \ell \nu_\ell$ and $D \rightarrow K \ell \nu_\ell$ from QCD Light-Cone Sum Rules, *Phys. Rev. D* **80** (2009) 114005. [[arXiv:0907.2842](#)]
- [60] G. Duplancic, A. Khodjamirian, T. Mannel, B. Melic and N. Offen, Light-cone sum rules for $B \rightarrow \pi$ form factors revisited, *JHEP* **04** (2008) 014. [[arXiv:0801.1796](#)]
- [61] D. D. Hu, H. B. Fu, T. Zhong, L. Zeng, W. Cheng and X. G. Wu, $\eta^{(\prime)}$ -meson twist-2 distribution amplitude within QCD sum rule approach and its application to the semi-leptonic decay $D_s^+ \rightarrow \eta^{(\prime)} \ell^+ \nu_\ell$, *Eur. Phys. J. C* **82** (2022) 12. [[arXiv:2102.05293](#)]
- [62] T. Huang, B. Q. Ma and Q. X. Shen, Analysis of the pion wave function in light cone formalism, *Phys. Rev. D* **49** (1994) 1490. [[hep-ph/9402285](#)]
- [63] X. G. Wu and T. Huang, An implication on the pion distribution amplitude from the pion-photon transition form factor with the new BABAR data, *Phys. Rev. D* **82** (2010) 034024. [[arXiv:1005.3359](#)]
- [64] X. G. Wu and T. Huang, Constraints on the light pseudoscalar meson distribution amplitudes from their meson-photon transition form factors, *Phys. Rev. D* **84** (2011) 074011. [[arXiv:1106.4365](#)]
- [65] F. G. Cao and T. Huang, Large corrections to asymptotic $F(\eta_c \gamma)$ and $F(\eta_b \gamma)$ in the light cone perturbative QCD, *Phys. Rev. D* **59** (1999) 093004. [[hep-ph/9711284](#)]
- [66] T. Huang and X. G. Wu, A model for the twist-3 wave function of the pion and its contribution to the pion form-factor, *Phys. Rev. D* **70** (2004) 093013. [[hep-ph/0408252](#)]
- [67] X. G. Wu and T. Huang, Pion electromagnetic form-factor in the k_T factorization formulae, *Int. J. Mod. Phys. A* **21** (2006) 901. [[hep-ph/0507136](#)]
- [68] T. Zhong, Z. H. Zhu, H. B. Fu, X. G. Wu and T. Huang, Improved light-cone harmonic oscillator model for the pionic leading-twist distribution amplitude, *Phys. Rev. D* **104** (2021) 016021. [[arXiv:2102.03989](#)]
- [69] S. J. Brodsky and G. F. de Teramond, Hadronic spectra and light-front wavefunctions in holographic QCD, *Phys. Rev. Lett.* **96** (2006) 201601. [[hep-ph/0602252](#)];
- [70] S. J. Brodsky and G. F. de Teramond, Light-Front dynamics and AdS/QCD correspondence: the pion form factor in the space- and time-like regions, *Phys. Rev. D* **77** (2008) 056007. [[arXiv:0707.3859](#)]
- [71] S. J. Brodsky and G. F. de Teramond, AdS/CFT and Light-Front QCD, *Subnucl. Ser.* **45** (2009) 139-183 [[arXiv:0802.0514](#)]
- [72] T. Zhong, X. G. Wu, J. W. Zhang, Y. Q. Tang and Z. Y. Fang, New results on Pionic Twist-3 Distribution Amplitudes within the QCD Sum Rules, *Phys. Rev. D* **82** (2010) 034024. [[arXiv:1101.3592](#)]
- [73] X. H. Guo and T. Huang, Hadronic wave functions in D and B decays, *Phys. Rev. D* **43** (1991) 2931-2938.
- [74] H. B. Fu, X. G. Wu, H. Y. Han, Y. Ma and T. Zhong, $|V_{cb}|$ from the semileptonic decay $B \rightarrow D \ell \bar{\nu}_\ell$ and the properties of the D meson distribution amplitude, *Nucl. Phys. B* **884** (2014) 172-192. [[arXiv:1309.5723](#)]
- [75] P. A. Zyla et al. (Particle Data Group), Review of Particle Physics, *Prog. Theor. Exp. Phys.* **2020** (2020) 083C01.
- [76] M. A. Shifman, Wilson loop in vacuum fields, *Nucl. Phys. B* **173** (1980) 13-31.
- [77] S. Narison, Improved $f_{D(s)^*}, f_{B(s)^*}$ and f_{B_c} from QCD Laplace sum rules, *Int. J. Mod. Phys. A* **30** (2015) 1550116. [[arXiv:1404.6642](#)]
- [78] P. Colangelo and A. Khodjamirian, QCD sum rules, a modern perspective, [[hep-ph/0010175](#)]
- [79] M. Ablikim et al. [BES Collaboration], Direct measurements of the branching fractions for $D^0 \rightarrow K^- e^+ \nu(e)$ and $D^0 \rightarrow \pi^- e^+ \nu_e$ and determinations of the form-factors $f_+^K(0)$ and $\pi_+(0)$, *Phys. Lett. B* **597** (2004) 39-46. [[hep-ex/0406028](#)].
- [80] P. Ball, Testing QCD sum rules on the light-cone in $D \rightarrow (\pi, K) \ell \nu$ decays, *Phys. Lett. B* **641** (2006) 50-56 [[hep-ph/0608116](#)].
- [81] A. Bharucha, D. M. Straub and R. Zwicky, $B \rightarrow V \ell^+ \ell^-$ in the Standard Model from light-cone sum rules, *JHEP* **08** (2016) 098 [[arXiv:1503.05534](#)]
- [82] H. J. Tian, H. B. Fu, T. Zhong, X. Luo, D. D. Hu and Y. L. Yang, Investigating the $D_s^+ \rightarrow \pi^0 \ell^+ \nu_\ell$ decay process within the QCD sum rule approach, *Phys. Rev. D* **108** (2023) 076003. [[arXiv:2306.07595](#)]
- [83] J. L. Hewett, Searching for new physics with charm, [hep-ph/9505246](#).
- [84] M. Golz, Physics reach of $D_{(s)} \rightarrow \pi(K) \ell \ell$ and other charming null test opportunities, [[arXiv:2105.03453](#)].